Energy Transfer in Molecular Dyads Comprising Metalloporphyrin and Ruthenium(II) Tris(2,2′-bipyridyl) Terminals. Competition between Internal Conversion and Energy Transfer in the Upper Excited Singlet State of the Porphyrin

Anthony Harriman,* Muriel Hissler, Olivier Trompette, and Raymond Ziessel*

Contribution from the Laboratoire de Chimie, d'Electronique et de Photonique Moléculaires, Ecole Européenne de Chimie, Polymères et Matériaux, Université Louis Pasteur, UPRES-A 7008 au CNRS, 25 rue Becquerel, 67087 Strasbourg Cedex 02, France

Received July 1, 1998

Abstract: The photophysical properties of a tripartite supermolecule comprising zinc porphyrin and ruthenium(II) tris(2,2′-bipyridyl) terminals separated by a trans Pt^{II} bis-*σ*-acetylide fragment bearing tri-*n*-butylphosphine residues have been recorded in solution. Thus, excitation into the ruthenium(II) tris(2,2′-bipyridyl) fragment is followed by fast intramolecular energy transfer to the triplet state of the porphyrin with only a minor contribution from competing (spin-forbidden) triplet-to-singlet energy transfer. Deactivation of the first excited singlet state localized on the porphyrin involves singlet-to-triplet energy transfer to populate the triplet state of the ruthenium(II) tris(2,2′-bipyridyl) complex, which rapidly transfers excitation energy to the triplet state of the porphyrin. There is no experimental evidence in support of intramolecular electron transfer between the terminals, such processes being inhibited by poor thermodynamics and by the barrier imposed by the central Pt^{II} bis-*σ*-acetylide fragment. Following excitation into the second excited singlet state of the porphyrin moiety, which has an inherent lifetime of ca. 3 ps, ultrafast singlet-to-singlet energy transfer to the ruthenium(II) tris(2,2′-bipyridyl) complex competes with internal conversion. Rapid intersystem crossing within the excited-state manifold of the ruthenium(II) tris(2,2′-bipyridyl) fragment is then followed by slower triplet energy transfer to the porphyrin.

Many elaborate photoactive molecular dyads,[1] triads,[2] and higher order arrays[3] have been designed and studied in recent years. Such supermolecules are intended to display vectorial energy and/or electron transfer along the molecular axis upon selective illumination into a preferred chromophore. Clearly, the choice of material that connects the photoactive subunits is of prime importance and, for effective intramolecular transfer of stored information, it is necessary that the connector promotes either through-bond or through-space interactions. The connector must also be sufficiently versatile to enable construction of different (with respect to size, shape, composition, and organization) supermolecules. This latter requisite is best achieved via a modular synthetic approach in which the supermolecule is assembled from preformed units by way of noncovalent interactions.[4,5] In this regard, coordination of functionalized polytopic ligands around a metallo-fragment provides an especially appealling method for assemblage of multicomponent systems.[6]

One of several modes available for building such intricate structures around a metal center is to benefit from the square-

(1) For leading references, see: (a) Connolly, J. S.; Bolten, J. R. In *Photoinduced Electron Transfer*; Fox, M. A., Channon, M., Eds.; Elsevier: Amsterdam, 1988; Part D, p 303. (b) Gust, D.; Moore, T. A. *Science* **1989**, *244*, 35. (c) Maruyama, K.; Osuka, A. *Pure Appl. Chem.* **1990**, *62*, 1511. (d) Wasielewski, M. R. *Chem. Rev.* **1992**, *62*, 1511. (e) Brun, A. M.; Harriman, A.; Heitz, V.; Sauvage, J.-P. *J. Am. Chem. Soc*. **1991**, *113*, 8657. (f) Oliver, A. M.; Craig, D. C.; Paddon-Row, M. N.; Kroon, J.; Verhoeven, J. *Chem. Phys. Lett*. **1988**, *150*, 366. (g) Yonemoto, E. H.; Riley, R. L.; Kim, Y. I.; Atherton, S. J.; Schmehl, R. H.; Mallouk, T. E. *J. Am. Chem. Soc*. **1992**, *114*, 8081. (h) DeGraziano, J. M.; Liddell, P. A.; Leggett, L.; Moore, A. L.; Moore, T. A.; Gust, D. *J. Phys. Chem*. **1994**, *98*, 1758. (i) Benniston, A. C.; Harriman, A. *J. Am. Chem. Soc*. **1994**, *116*, 11531. (j) Indelli, M. T.; Bignozzi, C. A.; Harriman, A.; Schoonover, J. R.; Scandola, F. *J. Am. Chem. Soc*. **1994**, *116*, 3768. (k) Brun, A. M.; Harriman, A.; Tsuboi, Y.; Okada, T.; Mataga, N. *J. Chem. Soc., Faraday Trans*. **1995**, *91*, 4047. (l) Sessler, J. L.; Wang, B.; Harriman, A. *J. Am. Chem. Soc*. **1995**, *117*, 704. (m) Imahori, H.; Hagiwara, K.; Oki, M.; Akiyama, T.; Taniguchi, S.; Okada, T.; Shirakawa, M.; Sakata, Y. *J. Am. Chem. Soc*. **1996**, *118*, 11771.

(2) For leading references, see: (a) Gust, D.; Moore, T. A.; Liddell, P. A.; Nemeth, G. A.; Makings, L. R.; Moore, A. L.; Barrett, D.; Pessiki, P. J.; Bensasson, R. V.; Rougée, M.; Chachaty, C.; De Schryver, F. C.; Van der Auweraer, M.; Holzwarth, A. R.; Connolly, J. S. *J. Am. Chem. Soc.* **1987**, *109*, 846. (b) Wasielewski, M. R.; Gaines, G. L., III; O'Neil, M. P.; Svec, W. A.; Niemczyk, M. P. *J. Am. Chem. Soc*. **1990**, *112*, 4560. (c) Brouwer, A. M.; Eijckelhoff, C.; Willemse, R. J.; Verhoeven, J. W.; Schuddeboom, W.; Warman, J. M. *J. Am. Chem. Soc*. **1993**, *115*, 2988. (d) Gubelmann, M.; Harriman, A.; Lehn, J.-M.; Sessler, J.-L. *J. Phys. Chem*. **1990**, *94*, 308. (e) Benniston, A. C.; Harriman, A. *Angew. Chem., Int. Ed. Engl*. **1993**, *32*, 1459. (f) Ohkohchi, M.; Takahashi, A.; Mataga, N.; Okada, T.; Osuka, A.; Yamada, H.; Maruyama, K. *J. Am. Chem. Soc*. **1993**, *115*, 12137. (g) Gozstola, D.; Yamada, H.; Wasielewski, M. R. *J. Am. Chem. Soc*. **1995**, *117*, 2041. (h) van Dijk, S. I.; Wiering, P. G.; Groen, C. P.; Brouwer, A. N.; Verhoeven, J. W.; Schuddeboom, W.; Warman, J. M. *J. Chem. Soc., Faraday Trans*. **1995**, *91*, 2107. (i) Hung, S.-C.; Macpherson, A. N.; Lin, S.; Liddell, P. A.; Seely, G. R.; Moore, A. L.; Moore, T. A.; Gust, D. *J. Am. Chem. Soc*. **1995**, *117*, 1657. (j) Osuka, A.; Marumo, S.; Mataga, N.; Taniguchi, S.; Okada, T.; Yamazaki, I.; Nishimura, Y.; Ohno, T.; Nozaki, K. *J. Am. Chem. Soc*. **1996**, *118*, 155.

(3) (a) Van Patten, P. G.; Shreve, A. P.; Lindsey, J. S.; Donohoe, R. J. *J. Phys. Chem. B* **1998**, *102*, 4209. (b) Osuka, A.; Nakajima, S.; Maruyama, K.; Mataga, N.; Asahi, T.; Yamazaki, I.; Nishimura, Y.; Ohno, T.; Nozaki, K. *J. Am. Chem. Soc*. **1993**, *115*, 4577. (c) Gust, D.; Moore, T. A.; Moore, A. L.; Macpherson, A. N.; Lopez, A.; DeGraziano, J. M.; Gouni, I.; Bittersmann, E.; Seely, G. R.; Gao, F.; Nieman, R. A.; Ma, X. C.; Demanche, L. J.; Hung, S.-C.; Luttrull, D. K.; Lee, S.-J.; Kerrigan, P. K. *J. Am. Chem. Soc*. **1993**, *115*, 11141. (d) Sessler, J. L.; Capuano, V. L.; Harriman, A. *J. Am. Chem. Soc*. **1993**, *115*, 4618.

(4) Harriman, A.; Sauvage, J.-P. *Chem. Soc. Rev*. **1996**, 41.

(5) Harriman, A.; Ziessel, R. *Chem. Commun*. **1996**, 1707.

10.1021/ja982300a CCC: $18.00
Published on Web 03/05/1999

planar geometric requirements of alkynylated platinum(II) bis-phosphine complexes.[7] Here, the alkyne can be attached directly to Pt^{II}, with both trans and cis isomers being readily available.[8] The other end of the carbon chain can be functionalized with a suitable ligand that allows attachment of various redox-active or photoactive units.[9] We herein demonstrate the feasibility of this approach by reference to a tripartite supermolecule comprising zinc porphyrin and ruthenium(II) tris(2,2′-bipyridyl) terminals separated by a trans Pt^{II} bis-σ-acetylide fragment bearing tri-*n*-butylphosphine residues. These terminals have been selected for their complementary optical properties which permit selective excitation into either chromophore and because light-induced electron-transfer processes are unlikely to compete with energy transfer between the various states.

The main purpose of this investigation, however, is to explore the possibility of driving a photoreaction from an upper excited state in a molecular dyad. In this respect, it is important to note that the intense metal-to-ligand, charge-transfer absorption bands localized on the ruthenium(II) tris(2,2′-bipyridyl) ("Ru(bpy)") fragment are nicely positioned between the first and second excited singlet states associated with the zinc porphyrin. Indeed, these absorption bands seem well sited for the Ru^{II} complex to act as an energy acceptor for photons absorbed by the Soret band of the porphyrin, provided the donor excited state is sufficiently long-lived. From earlier steady-state fluorescence polarization studies and quantum yield determinations[10] it is known that the S_2 level of zinc(II) *meso*-tetraphenylporphyrin (ZnTPP) has a lifetime of ca. 3 ps. Metallophthalocyanines are also known[11] to possess relatively long-lived upper excited states, and recent measurements suggest that, for such compounds, S_2 might survive for 10 ps or so. The S_2 lifetime of ZnTPP was measured recently by fluorescence upconversion spectroscopy, and values of 3.5 and 2.4 ps, respectively, were found in acetonitrile[12] and ethanol.[13] Time-resolved anisotropy measurements made for the S_2 state are in good agreement with the earlier steady-state experiments, and it has been demonstrated[13] that vibrational relaxation within the S_1 level is much faster than conversion of S_2 into S_1. It was further shown[12] that S_2 transfers an electron to CH_2Cl_2 with an apparent bimolecular rate constant of ca. 10^{12} M^{-1} s^{-1} under conditions where S_1 remains inert. These realizations suggest that there could be interesting photochemistry occurring from upper excited states in closely spaced molecular dyads. In fact, related studies[14] have reported that energy transfer occurs from the S_2 level of a carotene to a covalently linked tetrapyrrolic pigment, despite the fact that the lifetime of the donor is only ca. 200 fs.

It has also been shown[15] that the Pt^{II} bis-σ-acetylide connector does not promote strong electronic coupling between attached terminals and that through-bond interactions are minimized. Such properties might favor through-space interactions, and, in particular, energy transfer is likely to take place via dipole−dipole interactions. Although other dyads formed from metalloporphyrin and ruthenium(II) polypyridine chromophores have been described,[16] none have been used to address the issue of whether or not the S_2 state can drive new photoprocesses.

Experimental Section

Full details for the synthesis, purification, and characterization of all new compounds studied here are provided in the Supporting Information. Structures of new compounds were authenticated by ^1H and ^{31}P NMR spectroscopy, FAB mass spectrometry, FT-IR, UV−visible absorption spectroscopy, and elemental composition. The instrumentation used to record steady-state and time-resolved laser spectroscopic properties of the various compounds is also fully described in the Supporting Information. The methodology used to derive rate constants for Förster dipole−dipole energy transfer is included in the Supporting Information, as is a description of the cyclic voltammetry setup used to measure reduction potentials.

Results and Discussion

Synthesis. The various multicomponent molecular systems were prepared as illustrated in Scheme 1 by a stepwise procedure based on the use of preformed metallo-synthons.[9] The key intermediate **2** was obtained in good yield by reaction of an ethynyl-grafted porphyrin with *trans*-$[Pt^{II}(P^nBu_3)_2Cl_2]$ in the presence of CuI as catalyst and diisopropylamine as base, following procedures described previously for σ-acetylide complexes.[8] The linear bis-porphyrin **1** and the analogous ruthenium tris(2,2′-bipyridyl)−porphyrin complex **3** were synthesized under similar conditions. On the basis of ^{31}P NMR spectral data (chemical shift around +4 ppm, with $J_{PPt} \approx 2300$ Hz) collected in solution and on FT-IR spectra recorded for the solid state ($\nu_{Pt-C\equiv C} \approx 2090$ cm^{-1}), we conclude that the central σ-ethynyl−platinum core retains the trans conformation upon incorporation into the various multicomponent species. No thermal or photochemical isomerization is expected for these complexes,[17] and, in fact, no such processes could be detected during steady-state or pulsed illumination.

General Properties of Complex 3. The absorption spectrum recorded for the tripartite complex **3** in acetonitrile (Figure 1) shows three prominent features of interest to the present investigation. The Q-band region, corresponding to the first excited singlet state of ZnP, is easily recognized between 500 and 600 nm while the intense metal-to-ligand, charge-transfer (MLCT) transition localized on the "Ru(bpy)" fragment is centered around 470 nm, where there is little absorption by ZnP. The Soret band of ZnP is seen as a very intense transition centered at 426 nm. The visible region of the spectrum is well reproduced by adding the individual contributions of selected molecular fragments (i.e., **2** + **4**), indicating the absence of pronounced electronic coupling between the terminal units. Other features can be discerned in the UV−visible spectrum,

(6) Romero, F. M.; Ziessel, R.; Von Dorsselaer, A.; Dupont-Cervais, A. *Chem. Commun*. **1996**, 551.

(7) (a) Mackay, L. G.; Anderson, H. L.; Sanders, J. K. M. *J. Chem. Soc., Chem. Commun*. **1992**, 43. (b) Sonogashira, K.; Yatake, T.; Tohda, Y.; Takahashi, S.; Hagihara, N. *J. Chem. Soc., Chem. Commun*. **1977**, 291. (c) Takahashi, S.; Kariya, M.; Yatake, T.; Sonogashira, K.; Hagihara, N. *Macromolecules* **1978**, *11*, 1063. (d) Faust, R.; Diederich, F.; Gramlich, V.; Seiler, P. *Chem.—Eur. J*. **1995**, *1*, 111.

(8) Hissler, M.; Ziessel, R. *J. Chem. Soc., Dalton Trans*. **1995**, 893.

(9) Hissler, M.; Ziessel, R. *New J. Chem*. **1997**, *21*, 847.

(10) Kurabayashi, Y.; Kikuchi, K.; Kokubun, H.; Kaizu, Y.; Kobayashi, H. *J. Phys. Chem*. **1984**, *88*, 1308.

(11) (a) Zhong, Q.; Wang, Z.; Liu, Y.; Zhu, Q.; Kong, F. *J. Chem. Phys*. **1996**, *105*, 5377. (b) Howe, L.; Zhang, J. Z. *J. Phys. Chem. A* **1997**, *101*, 3207.

(12) Chosrowjan, H.; Tanigichi, S.; Okada, T.; Takagi, S.; Arai, T.; Tokumaru, K. *Chem. Phys. Lett*. **1995**, *242*, 644.

(13) Gurzadyan, G. G.; Tran-Thi, T.-H.; Gustavsson, T. *J. Chem. Phys*. **1998**, *108*, 385.

(14) (a) Gust, D.; Moore, T. A.; Moore, A. L.; Devadoss, C.; Liddell, P. A.; Hermant, R.; Nieman, R. A.; Demanche, L. J.; DeGraziano, J. M.; Gouni, I. *J. Am. Chem. Soc*. **1992**, *114*, 3590. (b) Debreczeny, M. P.; Wasielewski, M. R.; Shinoda, S.; Osuka, A. *J. Am. Chem. Soc*. **1997**, *119*, 6407.

(15) Grosshenny, V.; Harriman, A.; Hissler, M.; Ziessel, R. *J. Chem. Soc., Faraday Trans*. **1996**, *92*, 2223.

(16) (a) Hamilton, A. D.; Rubin, H.-D.; Bocarsly, A. B. *J. Am. Chem. Soc*. **1984**, *106*, 7255. (b) Sessler, J. L.; Capuano, V. L.; Burrell, A. K. *Inorg. Chim. Acta* **1993**, *204*, 93. (c) Collin, J.-P.; Harriman, A.; Heitz, V.; Odobel, F.; Sauvage, J.-P. *J. Am. Chem. Soc*. **1994**, *116*, 5679. (d) Araki, K.; Toma, H. E. *J. Photochem. Photobiol. A: Chem*. **1994**, *83*, 245. (e) Collin, J.-P.; Harriman, A.; Heitz, V.; Odobel, F.; Sauvage, J.-P. *Coord. Chem. Rev*. **1996**, *148*, 63.

(17) Harriman, A.; Hissler, M.; Ziessel, R.; De Cian, A.; Fisher, J. *J. Chem. Soc., Dalton Trans*. **1995**, 4067.

Scheme 1[a]

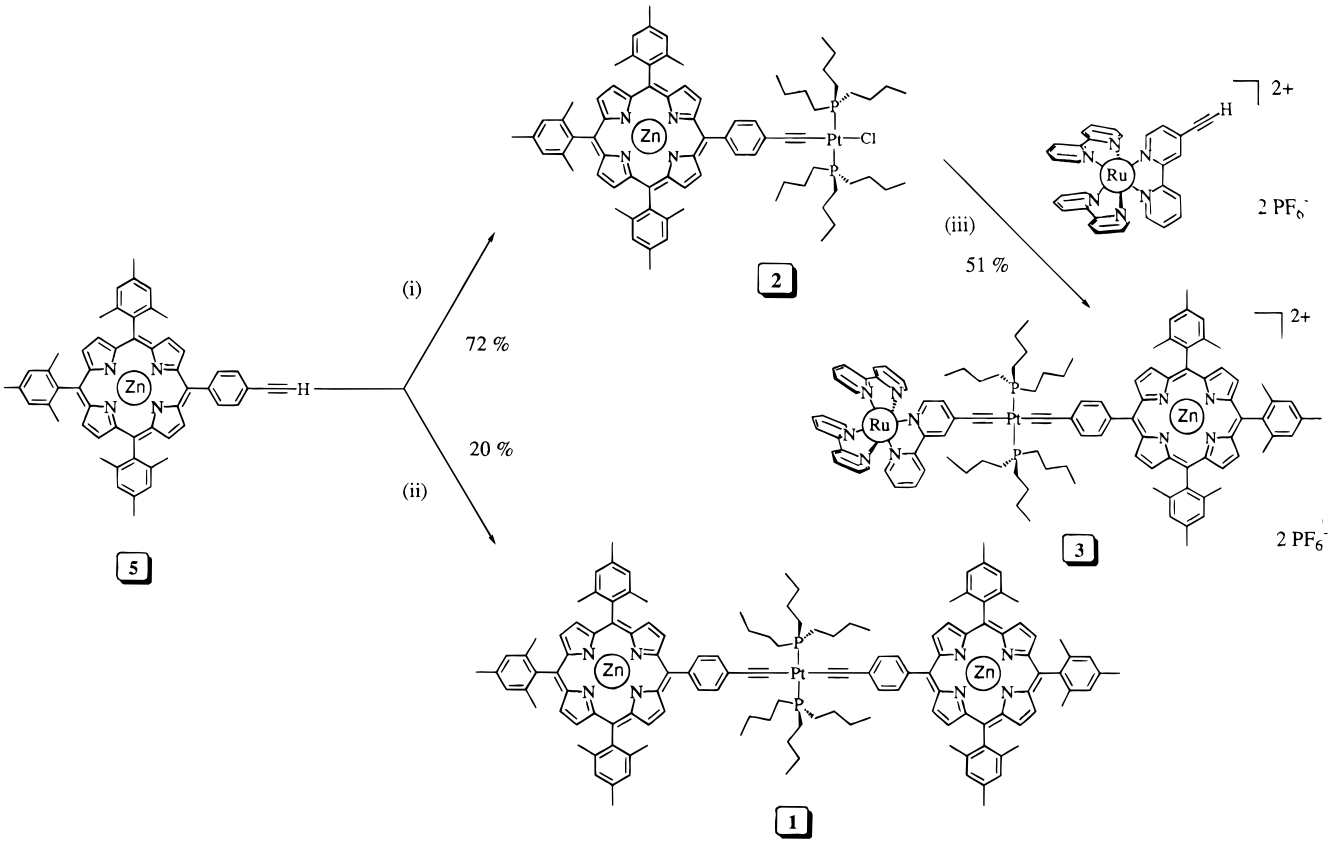

[a] (i) *trans*-[Pt(P^{n}Bu$_3$)$_2$Cl$_2$] 1 equiv, CuI 1%, (^{i}Pr)$_2$NH, THF, 25 °C, 7 days; (ii) *trans*-[Pt(P^{n}Bu$_3$)$_2$Cl$_2$] 0.5 equiv, CuI 1%, (^{i}Pr)$_2$NH, THF, 25 °C, 7 days; (iii) CuI 1%, CH_3CN, (^{i}Pr)$_2$NH, 25 °C, 3 days.

notably contributions from π,π^* transitions localized on 2,2′-bipyridyl ligands seen around 290 nm and the charge-transfer transition[18] associated with the Pt^{II} bis-acetylide connector centered around 350 nm.

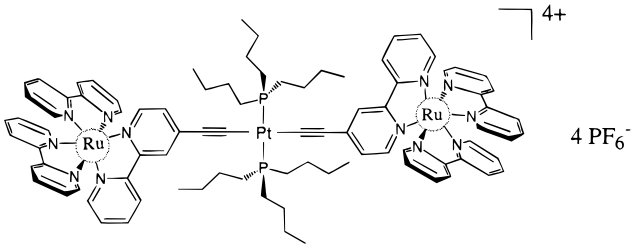

Cyclic voltammetry studies made with **3** in *N*,*N*-dimethylformamide indicate a series of quasi-reversible peaks that can be assigned by reference to the simpler systems **2** and **4** and for which half-wave potentials (E_{OX} or E_{RED}) can be established. Thus, ZnP is oxidized in a one-electron process ($E_{OX} = 0.82$ V vs SCE) to give the corresponding π-radical cation. The metal center present in the "Ru(bpy)" fragment undergoes a one-electron oxidation step ($E_{OX} = 1.35$ V vs SCE) at higher potential. Comparison with model compounds containing the alkyne function but lacking the Pt^{II} fragment (Scheme 1) indicates that the central Pt^{II} complex does not affect the ease of oxidation of either metal center. Upon cathodic scans, the first electron ($E_{RED} = -1.26$ V vs SCE) is added to the "Ru-(bpy)" fragment while the second and third electrons are added simultaneously ($E_{RED} = -1.42$ V vs SCE) to the porphyrin and "Ru(bpy)" fragment. The fourth electron ($E_{RED} = -1.70$ V vs SCE) is also added to the "Ru(bpy)" fragment while the fifth electron ($E_{RED} = -1.83$ V vs SCE) generates the π-dianion of the porphyrin.

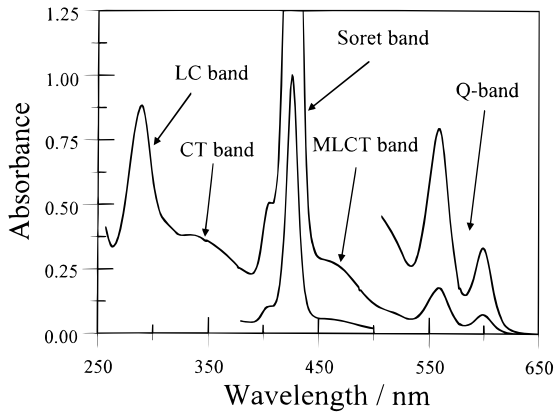

Figure 1. Absorption spectrum recorded for the tripartite compound **3** in acetonitrile solution. The Q-band and the Soret band are associated with the ZnP unit and refer, respectively, to promotion to the first and second excited singlet states. The metal-to-ligand, charge-transfer (MLCT) and ligand-centered (LC) transitions are localized on the "Ru(bpy)" fragment while the central Pt^{II} bis-σ-acetylide unit is responsible for the charge-transfer (CT) transition seen in the near-UV region.

Again, comparison can be made with the reduction of model compounds lacking the Pt^{II} fragment, and it is clear that the central Pt^{II} complex makes each terminal more difficult to reduce. Thus, from comparison of **5** and **2** (Scheme 1), these

(18) Masai, H.; Sonogashira, K.; Hagihara, N. *Bull. Chem. Soc. Jpn.* **1971**, *44*, 2226.

being models for the ZnP terminal, we find that the Pt^{II} fragment pushes E_{RED} for addition of the first electron from −1.22 to −1.39 V vs SCE. Similar effects have been noted previously for the "Ru(bpy)" terminal[15,17] and attributed to charge donation from the Pt^{II} center to the alkyne-bridged ligand. For the tripartite complex **3**, therefore, it is likely that the central Pt^{II} fragment donates charge to both ZnP and "Ru(bpy)" terminals. In fact, for the Pt-containing "Ru(bpy)"-based model compounds it was concluded that, under electrochemical conditions, charge donation to the alkyne-functionalized 2,2′-bipyridyl ligand is so pronounced that the first electron is added to one of the parent 2,2′-bipyridyl ligands.[15,19] This seems not to be the case for **3**, where the first electron is added to the alkyne-substituted 2,2′-bipyridine. We arrive at this conclusion because (i) reduction of the "Ru(bpy)" terminal has a small but definite effect on E_{RED} for the ZnP terminal and (ii) the difference between E_{RED} values for addition of one and two electrons to the "Ru(bpy)" terminal is unusually small and can be best explained in terms of the first electron being delocalized over the alkyne substituent.

The consequence of the first electron being localized at the alkyne-substituted 2,2′-bipyridine is of extreme importance since the lowest energy triplet excited state of the "Ru(bpy)" fragment involves charge transfer from metal center to the more readily reduced ligand.[20] In the model compounds, formation of the triplet state involves charge injection into one of the two parent ligands, but in **3** it will involve selective charge donation to the functionalized 2,2′-bipyridyl ligand, where it will be partially delocalized over the alkyne residue.[21] Such electron delocalization should assist intramolecular electron- or energy-transfer processes by directing charge toward the molecular axis.

Fluorescence from ZnP is readily detectable for **3** in acetonitrile at room temperature. This allows calculation of the energy of the first-excited singlet state of ZnP as being ca. 2.10 eV. Phosphorescence can be detected from ZnP in an ethanol glass at 77 K, from which the energy of the corresponding excited triplet state is determined to be ca. 1.62 eV. It is more difficult to estimate the triplet energy of the "Ru(bpy)" fragment since room temperature phosphorescence is hidden beneath fluorescence from ZnP. The phosphorescence spectrum becomes more evident at lower temperature, however, and is easily resolved at −50 °C. The triplet energy was subsequently estimated as being 2.00 eV by a spectral curve-fitting routine.[22] Taken together with the electrochemical data, these values permit estimation of thermodynamic driving forces ($\Delta G°$) for light-induced electron transfer between the terminals, calculated according to

$$\Delta G° = E_{OX} - E_{RED} - E_{ES} + \Delta E_C$$

$$\Delta E_C = \frac{\Delta Z e^2}{4\pi\epsilon_0\epsilon_S R} \qquad (1)$$

where E_{ES} is the electronic energy of the excited state, ΔZ is the difference in electronic charge between radical pair and initial reactants, ϵ_S is the static dielectric constant of the solvent, and R is the Zn−Ru cation−cation distance. The main results are collected in Table 1, calculated on the basis that $R = 23$ Å as deduced from MM2 energy-minimized, computer-modeling studies, and indicate that electron transfer is energetically unfavorable in all cases. Also included in Table 1 are estimates of the energy gap (ΔE) between the lowest energy electronic levels of the terminals, calculated according to

$$\Delta E = E_D - E_A \qquad (2)$$

where E_D and E_A refer, respectively, to the spectroscopic energy level of donor and acceptor measured in acetonitrile solution. It is apparent that the triplet excited state of ZnP forms an energy sink for this system.

Table 1. Calculated and Experimental Rate Constants for the Various Processes Expected to Take Place from the Lowest Energy Excited States Localized on the Terminals of the Tripartite Supermolecule **3** and the Appropriate Energy Gap or Driving Force for that Reaction

reaction	process[a]	ΔE ($\Delta G°$)/meV	$k/10^8$ s^{-1}
ZnP∼∼RuL^{*T} → ^{S}*ZnP∼∼RuL	T → S en tr	−100	<0.1[b]
ZnP∼∼RuL^{*T} → ^{T}*ZnP∼∼RuL	T → T en tr	380	2.0
ZnP∼∼RuL^{*T} → $^{\bullet+}$ZnP∼∼RuL$^{-\bullet}$	reductive el tr	100	nd[c]
ZnP∼∼RuL^{*T} → $^{\bullet-}$ZnP∼∼RuL$^{+\bullet}$	oxidative el tr	730	nd
^{S}*ZnP∼∼RuL → ZnP∼∼RuL*^{T}	S → T en tr	100	6.8[b]
^{S}*ZnP∼∼RuL → $^{\bullet+}$ZnP∼∼RuL$^{-\bullet}$	oxidative el tr	0	nd
^{S}*ZnP∼∼RuL → $^{\bullet-}$ZnP∼∼RuL$^{+\bullet}$	reductive el tr	610	nd
^{T}*ZnP∼∼RuL → ZnP∼∼RuL*^{T}	T → T en tr	−380	nd
^{T}*ZnP∼∼RuL → $^{\bullet+}$ZnP∼∼RuL$^{-\bullet}$	oxidative el tr	480	nd
^{T}*ZnP∼∼RuL → $^{\bullet-}$ZnP∼∼RuL$^{+\bullet}$	reductive el tr	1090	nd
^{S2}*ZnP∼∼RuL → ZnP∼∼RuL*^{S}	S → S en tr	530	3000[b]
^{S2}*ZnP∼∼RuL → $^{\bullet+}$ZnP∼∼RuL$^{-\bullet}$	oxidative el tr	−800	nd
^{S2}*ZnP∼∼RuL → $^{\bullet-}$ZnP∼∼RuL$^{+\bullet}$	reductive el tr	−190	nd

[a] en tr refers to energy transfer while el tr refers to light-induced electron transfer. [b] Calculated from Förster theory assuming the weak coupling limit. [c] Not detected.

Selective Excitation into the "Ru(bpy)" Metallo-Fragment. The MLCT absorption band associated with the "Ru(bpy)" subunit is well resolved in the absorption spectrum recorded for **3** in acetonitrile solution such that this chromophore can be preferentially excited within the range 440 nm < λ < 500 nm. Excitation of the reference compound **4** at 465 nm in deoxygenated acetonitrile gave rise to long-lived ($\tau_T = 1.30$ μs) phosphorescence centered around 625 nm, for which the quantum yield was found to be ca. 0.084. In marked contrast, illumination of the tripartite complex **3** under identical conditions gave rise to a luminescence spectrum that resembled fluorescence from ZnP contaminated with a small contribution (ca. 13%) of phosphorescence from the "Ru(bpy)" fragment (Figure 2a). The total emission quantum yield measured between 550 and 850 nm was ca. 0.002, indicating that luminescence from the "Ru(bpy)" fragment is heavily (i.e., ca. 95%) quenched in the tripartite system. Luminescence decay profiles, recorded at various wavelengths in the range 600−750 nm, could be well-represented in terms of a two exponential fit,

$$I_L(t) = A_1 \exp\left(-\frac{t}{\tau_1}\right) + A_2 \exp\left(-\frac{t}{\tau_2}\right) \qquad (3)$$

although the derived lifetimes ($\tau_1 = 1$ ns; $\tau_2 = 4$ ns) were too similar for accurate analysis (Figure 2b). The observed spectral variation of the fractional amplitudes (A_1 and A_2) was entirely consistent with the shorter-lived species being due to fluorescence from ZnP and with the longer-lived component being associated with phosphorescence from the "Ru(bpy)" fragment.

Quenching of the triplet excited state of the "Ru(bpy)" fragment could involve a combination of several processes (Table 1). Spectral overlap between phosphorescence from the

(19) Ziessel, R.; Hissler, M.; El-ghayoury, A.; Harriman, A. *Coord. Chem. Rev.* **1998**, *178−180*, 1251.
(20) Kalyanasundaram, K. In *Photochemistry of Polypyridine and Porphyrin Complexes*; Academic Press: London, 1992.
(21) Grosshenny, V.; Harriman, A.; Romero, F. M.; Ziessel, R. *J. Phys. Chem.* **1996**, *100*, 17472.
(22) Murtaza, Z.; Graff, D. K.; Zipp, A. P.; Worl, L. A.; Jones, W. E., Jr.; Bates, W. D.; Meyer, T. J. *J. Phys. Chem.* **1994**, *98*, 10504.

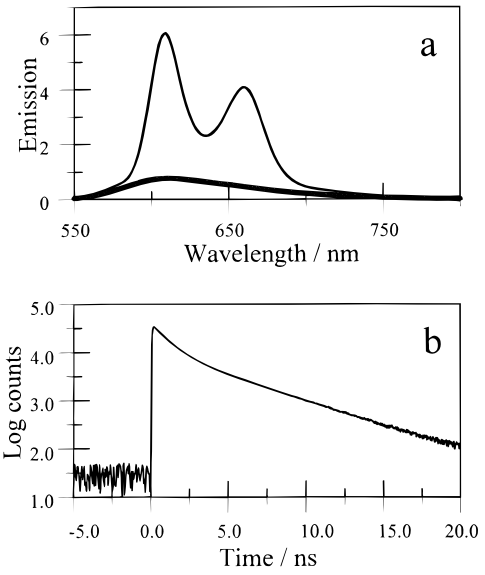

Figure 2. (a) Emission spectrum obtained on 465-nm excitation of **3** in deoxygenated acetonitrile. The curve drawn as a heavy line is the emission spectrum obtained after subtraction of the fluorescence spectrum of **2** and corresponds to phosphorescence from the "Ru(bpy)" fragment. Reconstruction of the observed spectrum shows that the latter process contributes ca. 13% of the total emitted photons over this spectral range. (b) Time-resolved emission profile recorded at 640 nm following laser excitation of **3** in deoxygenated acetonitrile at 460 nm, as measured using time-correlated, single-photon counting methodology.

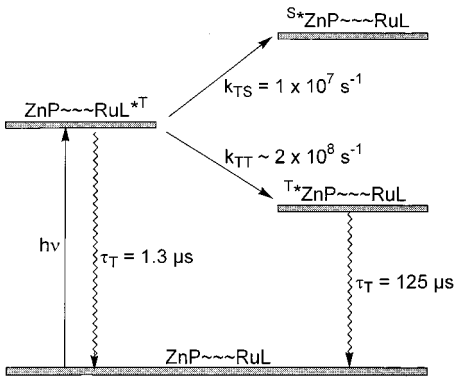

Figure 3. Simplified energy-level diagram showing the important processes involved in deactivation of the excited triplet state localized on the "Ru(bpy)" fragment of the supermolecule **3**. The rate constants and lifetimes refer to measured or calculated values while the inherent lifetime of the initial triplet state ($\tau_T = 1.3\ \mu s$) is equated to that of the reference compound **4**. The energy levels of the triplet states localized on "Ru(bpy)" and ZnP terminals, respectively, are 2.00 and 1.62 eV while that of the first excited singlet state of ZnP is 2.10 eV.

"Ru(bpy)" unit and absorption by the Q-band of ZnP corresponds to a Förster overlap integral of 1.95×10^{-14} mmol^{-1} cm^6. This value, when used together with the photophysical properties measured for **4**, provides an estimate for the rate of triplet-to-singlet energy transfer as being ca. 1.1×10^7 s^{-1}. However, comparison of the fluorescence excitation spectrum with the absorption spectrum shows no indication that light collected by the "Ru(bpy)" fragment is channeled to the singlet state of ZnP. Triplet-to-singlet energy transfer, therefore, is not expected to be a major contributor to the overall deactivation of the triplet state initially localized on the "Ru(bpy)" fragment (Figure 3). The observed fluorescence emanating from ZnP can be attributed to direct light absorption since the porphyrin absorbs about 5% of incident photons at 465 nm.

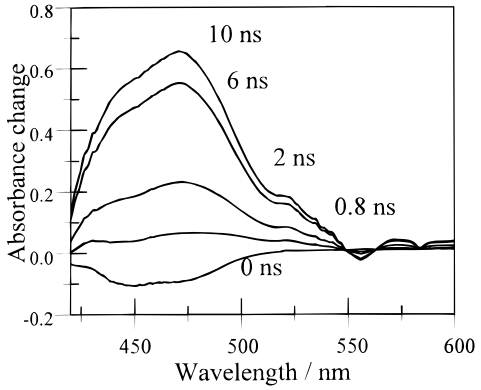

Figure 4. Differential absorption spectra recorded at various times after excitation of **3** in deoxygenated acetonitrile with a 20-ps laser pulse at 465 nm. The initial and final spectra refer, respectively, to the triplet excited states localized on the "Ru(bpy)" and ZnP terminals.

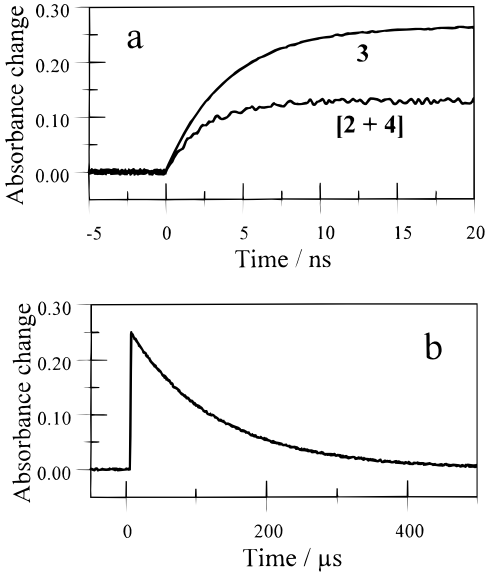

Figure 5. (a) Growth of absorbance at 845 nm following excitation with a 20-ps laser pulse at 465 nm, as measured with a fast-response photodiode. The signals correspond to excitation of **3** and an optically matched, equimolar mixture of **2** and **4**. The latter signal is shown at 10× amplification for clarity of presentation. (b) Decay of the absorbance at 845 nm measured for **3** on a long time scale.

Flash photolysis studies made with a 20-ps laser pulse at 465 nm, where the "Ru(bpy)" fragment is the dominant chromophore, showed the triplet excited state of this species to be present immediately after excitation (Figure 4). The triplet decayed with a lifetime of ca. 4 ns to leave behind a residual absorption spectrum possessing the characteristic features of the triplet excited state of ZnP. The yield of this latter species could be measured most conveniently at 845 nm, where other species make little contribution to the overall signal. Following laser excitation of an equimolar mixture of **2** and **4** in deoxygenated acetonitrile, prepared so as to possess an overall absorbance at 465 nm of 0.25, the transient absorbance at 845 nm (A_{845}) could be quantified by the following expression (Figure 5a):

$$A_{845} = A_0\left[\exp\left(-\frac{t}{\tau_T}\right) - \exp\left(-\frac{t}{\tau_{INST}}\right)\right]$$

$$A_0 = \alpha N_{ABS}\Phi_T\epsilon_T \qquad (4)$$

Here, the terms τ_{INST} (= 2.4 ns) and τ_T (= 125 μs) refer, respectively, to the response time of the photodiode used to

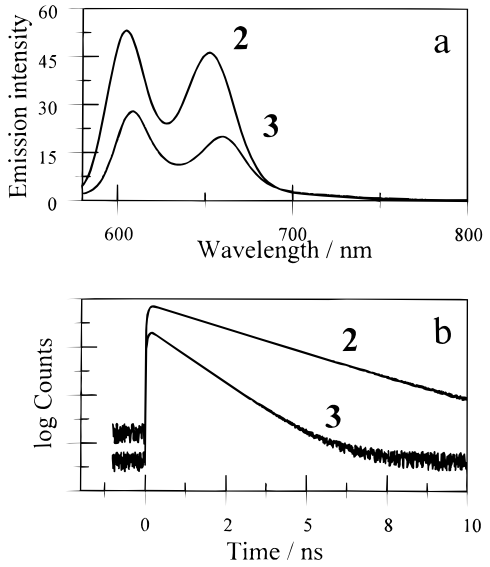

Figure 6. (a) Fluorescence spectra recorded following excitation of optically-matched acetonitrile solutions of **2** and **3**. The excitation wavelength was 565 nm, where ZnP is the dominant chromophore in **3**. (b) Time-resolved fluorescence decay profiles recorded following excitation of **2** and **3** in deoxygenated acetonitrile with a 6-ps laser pulse at 590 nm. One full division corresponds to 10 000 counts in the maximum channel.

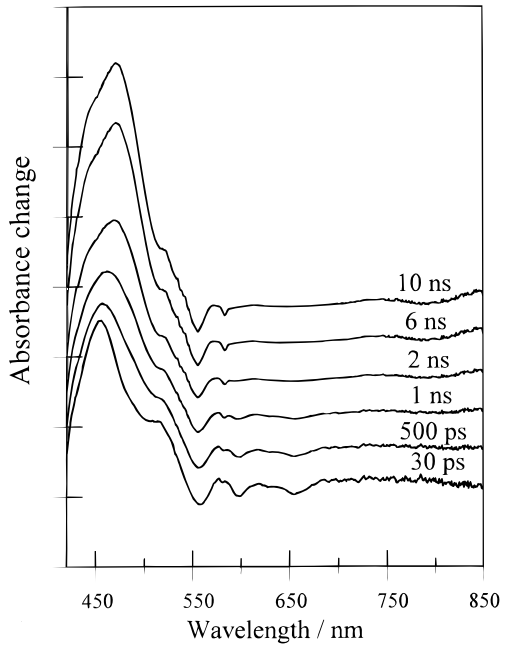

Figure 7. Differential absorption spectra recorded at various times after excitation of **3** in deoxygenated acetonitrile with a 20-ps laser pulse at 598 nm, with one division corresponding to an absorbance change of 0.1. The initial and final spectra refer, respectively, to the singlet and triplet excited states localized on ZnP.

monitor the signal and the triplet lifetime of ZnP, Φ_T (=0.88) is the quantum yield for formation of triplet ZnP by way of intersystem crossing from the singlet manifold, and ϵ_T (=8050 M^{-1} cm^{-1}) is the differential molar extinction coefficient for triplet ZnP at 845 nm. The total number of photons absorbed from the incident laser pulse at 465 nm (N_{ABS}) is a linear function of the laser intensity while the coefficient α (= 0.05) describes that fraction of the absorbed photon density harvested by ZnP.

Under identical experimental conditions, the transient absorbance at 845 nm measured for **3** could be quantified according to

$$A_{845} = (A_0 + B_0)\exp\left(-\frac{t}{\tau_T}\right) - A_0\exp\left(-\frac{t}{\tau_{INST}}\right) - B_0\exp\left(-\frac{t}{\tau_{Ru}}\right)$$

$$B_0 = (1-\alpha)N_{ABS}\epsilon_T T \qquad (5)$$

where τ_{Ru} (= 4 ns) refers to the triplet lifetime of the "Ru(bpy)" fragment. The term T (= 0.85 ± 0.07) corresponds to the efficiency of intramolecular triplet energy transfer from "Ru(bpy)" to ZnP (Figure 5). It follows that triplet-to-triplet energy transfer, which is spin-allowed and highly exothermic (ΔE = 0.38 eV), is essentially quantitative in this system and occurs with a rate constant of ca. 2×10^8 s^{-1}. The process is most likely due to Dexter-type electron exchange (Figure 3).

Excitation into the Q-Band of the ZnP Subunit. Illumination of **3** in acetonitrile at 565 nm, where the ZnP subunit is the dominant (i.e., >95%) chromophore, results in the appearance of fluorescence characteristic of the porphyrin. The fluorescence quantum yield ($\Phi_F = 0.022 \pm 0.002$), when compared to that measured for **2** ($\Phi_F = 0.042 \pm 0.002$), suggests that the excited singlet state of the ZnP subunit is quenched by ca. 50% (Figure 6a). Fluorescence decay profiles recorded after laser excitation at 590 nm, where ZnP is the sole chromophore, were monoexponential and corresponded to a singlet lifetime of 0.95 ± 0.08 ns (Figure 6b). Again, relative to the fluorescence lifetime measured for **2** (τ_S = 2.1 ns) under identical conditions, it is clear that the excited singlet state of ZnP in the tripartite complex **3** is quenched by ca. 50% due to the presence of the appended "Ru(bpy)" fragment (Figure 6b). The rate constant for this intramolecular quenching step can be estimated from the measured singlet lifetimes as being ca. 6×10^8 s^{-1}. According to the energy gaps listed in Table 1, the two most likely quenching processes involve oxidative electron transfer and singlet-to-triplet energy transfer. There is no thermodynamic driving force for light-induced electron transfer, and it is known from earlier work that the central Pt^{II} bis-σ-acetylide bridge imposes a barrier for through-bond electron exchange.[15] It is unlikely, therefore, that oxidative electron transfer plays a significant role in fluorescence quenching. However, Förster-type singlet-to-triplet energy transfer, despite the small overlap integral ($J_F = 4.2 \times 10^{-15}$ $mmol^{-1}$ cm^6), is expected to take place on the appropriate time scale, and the calculated rate constant ($k_F = 6.8 \times 10^8$ s^{-1}) is in excellent agreement with the experimental value.

Excitation of **3** in deoxygenated acetonitrile with a 20-ps laser pulse at 598 nm resulted in immediate formation of a transient differential absorption spectrum having the characteristic features[23] of the excited singlet state of ZnP (Figure 7). This species decayed over a few nanoseconds to form the triplet excited state of ZnP, as identified by its transient absorption spectral profile, which itself decayed slowly ($\tau_T \approx 125 \pm 25$ μs) to restore the prepulse baseline. Kinetic measurements made over the wavelength range $420 < \lambda < 520$ nm showed markedly nonlinear behavior (Figure 8a), and although the transient spectra do not contain intense bands attributable to an additional intermediate, it is clear that a third transient is involved in the overall process. Using the kinetic parameters extracted from these fits together with the model displayed in Figure 9, it becomes possible to

(23) (a) Rodriguez, J.; Kirmaier, C.; Holten, D. *J. Am. Chem. Soc.* **1989**, *111*, 6500. (b) Mataga, N.; Yao, H.; Okada, T.; Kanda, Y.; Harriman, A. *Chem. Phys.* **1989**, *131*, 473.

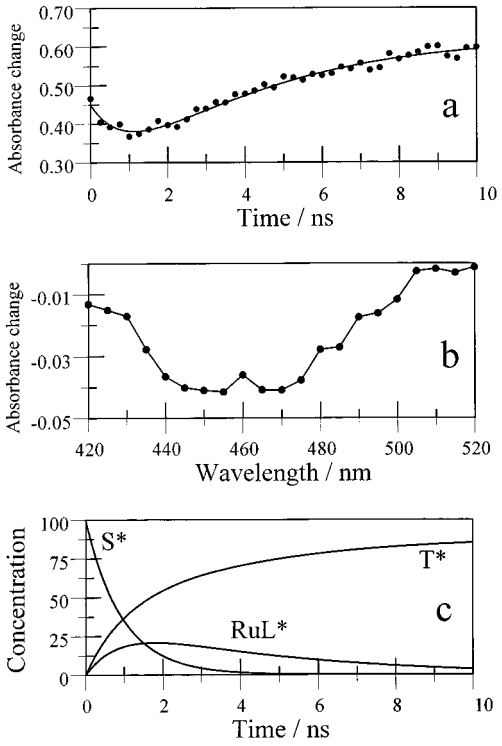

Figure 8. (a) Time profile of the differential absorbance measured at 450 nm following excitation of **3** in deoxygenated acetonitrile with a 20-ps laser pulse at 598 nm. The solid line drawn through the data points corresponds to a computer fit to the model discussed in the text where there is an intermediate species having a lifetime of 4 ns. (b) Differential absorption spectrum derived for the transient having an average lifetime of 4 ns, as measured at a delay time of 2.0 ns. This spectrum was obtained by subtracting the combined spectra due to excited singlet and triplet states associated with ZnP from the observed spectrum. The concentration of each ZnP-derived species was calculated from the initial and final spectra on the basis of the reaction scheme displayed in Figure 9. (c) Time dependence of the concentration of the excited singlet (S*) and triplet (T*) states localized on ZnP and the triplet state localized on the "Ru(bpy)" fragment (RuL*). These profiles were calculated by fitting the transient differential absorption spectra collected at various delay times between 0 and 10 ns to known spectra of the three species.

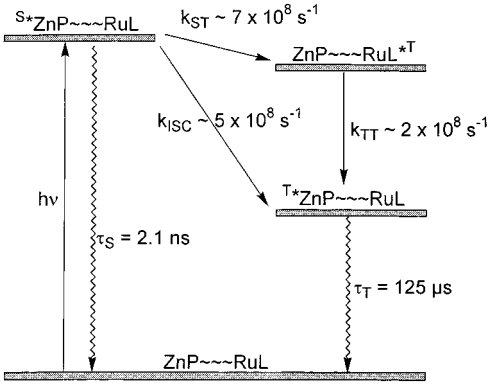

Figure 9. Simplified energy-level diagram showing the important processes involved in deactivation of the first excited singlet state localized on the ZnP terminal of the supermolecule **3**. The rate constants and lifetimes refer to measured or calculated values while the inherent lifetime of the singlet state (τ_S = 2.1 ns) is equated to that of the reference compound **2**. The energy levels of the various states are given in the legend to Figure 3.

compile a transient differential absorption spectrum for the species having a lifetime of 4 ns (Figure 8b). This species is

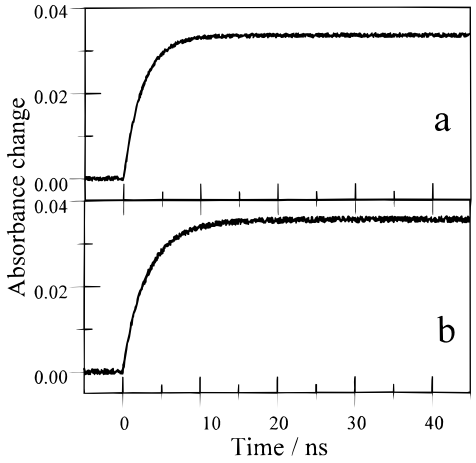

Figure 10. Growth of absorbance at 845 nm following excitation with a 20-ps laser pulse at 598 nm, as measured with a fast-response photodiode. The signals correspond to excitation of (a) an equimolar mixture of **2** and **4** and (b) an optically matched solution of **3** in deoxygenated acetonitrile.

easily identified as being the triplet excited state of the "Ru(bpy)" fragment. Furthermore, on the basis of known differential absorption spectra for the three species, the spectral records can be analyzed globally to monitor formation and decay of each species (Figure 8c). It becomes evident that the triplet excited state of the "Ru(bpy)" fragment builds up over ca. 1 ns and decays with a lifetime of 4 ns. The overall spectral changes are entirely consistent with a two-step, energy-transfer process in which the triplet excited state of the "Ru(bpy)" fragment functions as a relay to catalyze intersystem crossing within the ZnP excited-state manifold.

To quantify the yield of the ZnP triplet in these experiments, the transient absorbance was measured at 845 nm over long time scales using a photodiode as detector (Figure 10). Thus, excitation of an equimolar mixture of **2** and **4** in deoxygenated acetonitrile, prepared to have an absorbance of 0.08 at 598 nm, with a 20-ps laser pulse at 598 nm, where only **2** absorbs, gave the triplet excited state of the porphyrin. The differential absorbance recorded at 845 nm on long time scales could be quantitatively described as follows:

$$A_{845} = C_0\left[\exp\left(-\frac{t}{\tau_T}\right) - \exp\left(-\frac{t}{\tau_{INST}}\right)\right]$$

$$C_0 = N_{ABS}\Phi_T\epsilon_T \qquad (6)$$

where the photodiode response time is comparable to the lifetime of the excited singlet state of the porphyrin. Laser excitation of an optically matched solution of **3** under identical conditions also resulted in formation of the triplet excited state of ZnP, for which the differential absorbance at 845 nm could be described by the following expression:

$$A_{845} = D_0 \exp\left(-\frac{t}{\tau_T}\right) - (1-F)C_0 \exp\left(-\frac{t}{\tau_{INST}}\right) - \frac{FPC_0}{\Phi_T}\exp\left(-\frac{t}{\tau_{RU}}\right)$$

$$D_0 = C_0(1-F) + \frac{FPC_0}{\Phi_T}$$

$$F = \Phi_F/\Phi_F^\circ \qquad (7)$$

Here, Φ_F and Φ_F° refer, respectively, to the fluorescence

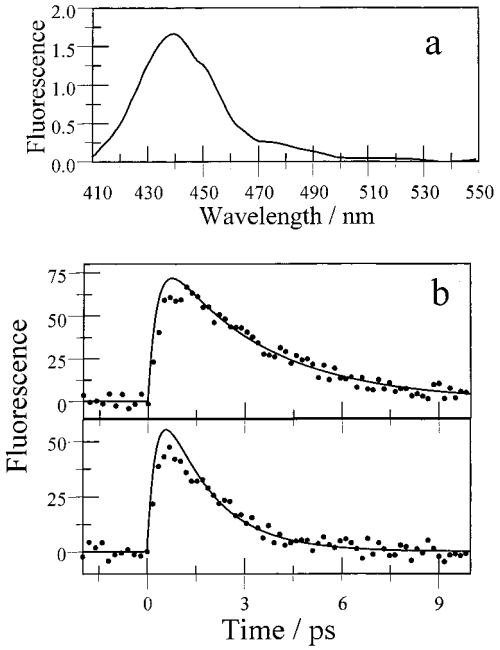

Figure 11. (a) Spectrum recorded for $S_2 \rightarrow S_0$ fluorescence observed from **3** in acetonitrile following excitation at 390 nm. (b) Decay profiles recorded for $S_2 \rightarrow S_0$ fluorescence observed for **2** (upper panel) and **3** (lower panel) following excitation with a 0.3-ps laser pulse at 420 nm. The solid curves drawn through the data points correspond to a rise time of ca. 0.4 ps and decay times of 3.1 and 1.4 ps, respectively, for **2** and **3**.

quantum yields recorded for **3** and **2**, and P is the probability that fluorescence quenching results in formation of the ZnP triplet. Analysis of the experimental data indicates that $P = 0.85 \pm 0.07$, confirming the earlier indication that triplet energy transfer from the Ru^{II} tris(2,2′-bipyridyl) fragment to ZnP is almost quantitative. The overall reaction pathway is illustrated in Figure 9.

Excitation into the Soret Band of the ZnP Subunit. Illumination of **2** and **3** in deoxygenated acetonitrile solution at 390 nm, this wavelength corresponding to an upper vibrational level of the second excited singlet state of ZnP, resulted in the appearance of very weak $S_2 \rightarrow S_0$ fluorescence centered around 440 nm (Figure 11a). Such behavior has been reported[10] earlier for a variety of metalloporphyrins and is a consequence of the relatively large energy gap between S_2 and S_1 excited states. From the Strickler−Berg expression,[24] the radiative rate constant for emission from S_2 was calculated to be 2.6×10^8 s^{-1} but the emission quantum yield was too weak to be estimated with much certainty. Using fluorescence upconversion spectroscopy the lifetime of the S_2 state was found to be 3 ± 1 ps, which is in very good agreement with prior estimates of the S_2 lifetime of ZnTPP made by fluorescence polarization[10] and by fluorescence upconversion spectroscopy.[12,13] These derived values permit estimation of the fluorescence quantum yield as being ca. 0.0008. It is important to note that the corrected fluorescence excitation spectrum recorded by monitoring fluorescence at 660 nm was in excellent agreement with the ground-state absorption spectrum recorded over the entire visible range. Emission from the S_2 state is too weak to perturb the excitation spectrum such that internal conversion from S_2 to S_1 is essentially quantitative. Following laser excitation of 2 at 410 nm the characteristic absorption spectral features of the S_1 state are apparent within the 20-ps laser pulse, indicating that thermal cooling within the

(24) Strickler, S. J.; Berg, R. A. *J. Chem. Phys.* **1962**, *37*, 814.

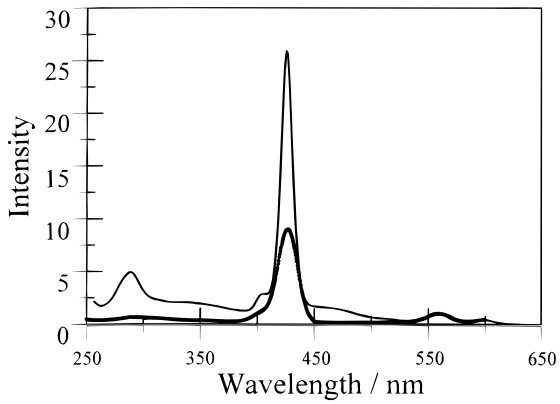

Figure 12. Correspondence between the absorption spectrum and corrected excitation spectrum (heavy curve) recorded for **3** in acetonitrile. The excitation spectrum was recorded for an optically dilute solution, monitoring emission at 660 nm, and the two spectra were normalized at 560 nm.

S_1 manifold is very fast. Similar conclusions have been raised for laser excitation of both ZnTPP[13] and metallophthalocyanines[11] (in the latter case the S_2 lifetime is ca. 10 ps) and for excitation of pyrene into high-energy singlet states.[25]

The lifetime of the S_2 state of **3**, as measured by fluorescence upconversion spectroscopy, was 1.5 ± 0.5 ps (Figure 11b). This finding, despite the large uncertainty limits, indicates that the S_2 state of **3** is involved in an additional photoprocess that competes with rapid $S_2 \rightarrow S_1$ internal conversion and that is not operative in **2**. Two other observations support this claim: First, it was found that the quantum yield for $S_1 \rightarrow S_0$ fluorescence was reduced by ca. 60% when excitation was made at 390 nm compared to 565 nm. Second, the corrected excitation spectrum recorded by monitoring $S_1 \rightarrow S_0$ emission at 660 nm did not match the absorption spectrum in the region around the Soret band (Figure 12). After normalization at 560 nm, it appears that only ca. 35% of photons absorbed by the Soret band are used to produce $S_1 \rightarrow S_0$ fluorescence, in marked contrast to the situation found for **2**. It is clear, therefore, that the S_2 state of ZnP in **3** is quenched on the time scale of a few picoseconds.

Because of an improved spectral overlap integral ($J_F = 4.5 \times 10^{-14}$ $mmol^{-1}$ cm^6) singlet-to-singlet energy transfer from S_2 to the "Ru(bpy)" fragment might be expected to compete with $S_2 \rightarrow S_1$ internal conversion. This process would generate the MLCT excited singlet state of the metal complex which, after rapid intersystem crossing to the triplet state, would populate the triplet state of ZnP via energy transfer with minimal involvement of the S_1 level of ZnP. Indeed, on the basis of photophysical properties of the S_2 state estimated for **2**, we calculate that the rate constant of Förster-type intramolecular energy transfer for **3** is ca. 3×10^{11} s^{-1}. This process, even allowing for the inherent uncertainty of the calculation, is on the appropriate time scale and is likely to be augmented by Dexter-type electron exchange since the spectral overlap integral for Dexter energy transfer ($J_D = 2.3 \times 10^{-4}$ cm) is relatively high.

Alternatively, the higher energy of the S_2 state could facilitate electron transfer to the "Ru(bpy)" terminal. This latter process is thermodynamically unfavorable in the case of S_1 ($\Delta G° \approx 0.0$ eV) but becomes more likely from S_2 ($\Delta G° \approx -0.8$ eV). Light-induced electron transfer should produce a radical ion pair which, because it is essentially isoenergetic with the S_1 level of ZnP, is expected to decay by way of populating the lower energy excited state.[26] However, it was found that the decay

(25) Foggi, P.; Corti, S.; Righini, R.; Califano, S. *AIP Conf. Proc.* **1996**, *364 (Elementary Processes in Chemical and Biological Systems)*, 169.

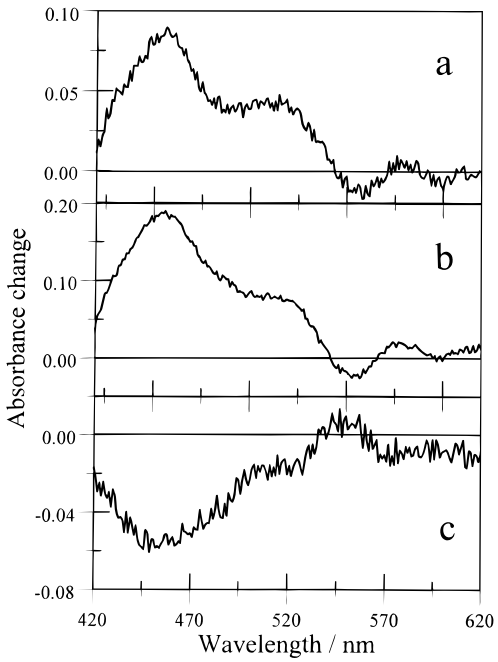

Figure 13. Differential absorption spectra recorded immediately after excitation of (a) **3** and (b) **2** in acetonitrile with a 20-ps laser pulse at 410 nm. Each spectrum was recorded at "zero time" where the excitation and probe pulses exhibit maximum overlap. Panel c shows the difference spectrum obtained by subtracting the spectrum obtained for **2** from that of **3**, using a global spectral curve fitting routine.

profile recorded for stimulated $S_1 \rightarrow S_0$ fluorescence remained monoexponential for laser excitation at both 598 and 410 nm. This observation shows that there is no reverse electron transfer to form S_1 and seems in line with an energy-transfer quenching mechanism.

Laser flash photolysis studies made for excitation of **3** with a 20-ps laser pulse at 410 nm indicate that the transient differential absorption spectrum generated within the excitation pulse contains contributions from both the excited singlet state of ZnP and the triplet state of the "Ru(bpy)" fragment (Figure 13). Comparison of transient spectra recorded for **3** at the center of the laser pulse for excitation at 598 and 410 nm clearly shows that the triplet state of the Ru^{II} complex is present in the latter case but not in the former. The same situation is seen by comparison of transient spectra recorded at early times following excitation of **2** and **3** with a 20-ps laser pulse at 410 nm. Although we lack the temporal resolution to monitor emergence of this signal, it is apparent that it must arise during decay of the S_2 state localized on ZnP. The laser flash photolysis records show no obvious component that can be assigned to an intermediate radical ion pair, and it seems unlikely that light-induced electron transfer plays a significant role in the overall photoprocesses, regardless of excitation wavelength. On much longer time scales, the transient spectroscopic records show emergence and subsequent decay of the triplet excited state of ZnP such that the reaction pathway is as illustrated in Figure 14.

Concluding Remarks

The tripartite supermolecule **3** shows a variety of intramolecular energy-transfer processes; namely, ultrafast singlet-to-singlet, fast triplet-to-triplet and singlet-to-triplet, and (perhaps)

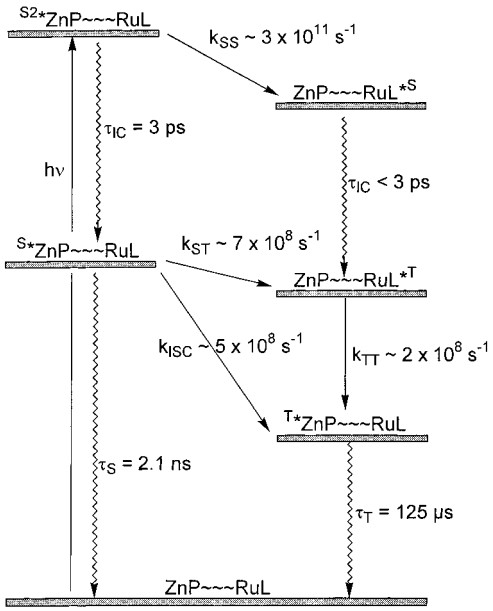

Figure 14. Simplified energy-level diagram showing the important processes involved in deactivation of the second excited singlet state localized on the ZnP terminal of the supermolecule **3**. The rate constants and lifetimes refer to measured or calculated values while the inherent lifetime of the upper excited singlet state ($\tau_{IC} = 3$ ps) is equated to that of the reference compound **2**. The energy of the S_2 level, taken from the intersection between absorption and fluorescence spectra, is 2.8 eV while the energy of the singlet MLCT state localized on the ruthenium(II) tris(2,2′-bipyridyl) fragment, estimated as the onset of the absorption profile, is ca. 2.27 eV. Other energy levels are given in the legend to Figure 3.

slow triplet-to-singlet. Absorption bands localized on the "Ru(bpy)" fragment nicely complement π,π^* transitions associated with ZnP, allowing Förster-type energy transfer to compete with internal conversion at the S_2 level of ZnP. As such, a cascade of energy-transfer processes is set up but essentially every photon absorbed by the supermolecule ends up in the triplet excited state of ZnP. The rate of (singlet-to-singlet) energy transfer from the S_2 level of ZnP is ca. 1000-fold faster than (singlet-to-triplet) energy transfer from the corresponding S_1 level, primarily because of an improved overlap integral. This ratio could easily be increased by modifying the optical properties of donor or acceptor. No other porphyrin-based molecular dyads are known that favor reactions from the porphyrin S_2 level rather than from S_1, but energy transfer from the S_2 level of carotenoids,[27] including porphyrin−carotene dyads,[14] is known. A drawback of the present system is that we are not obtaining a genuine benefit by switching on reactions from the S_2 level of ZnP, other than a faster rate, since a similar effect is achieved by excitation into the S_1 level. Improved prototypes, therefore, will need to ensure that new products can be engineered by selective excitation into the S_2 level.

The Pt^{II} bis-σ-acetylide bridge provides an interesting alternative to purely organic connectors; it is readily amenable to formation of cis or trans isomers, and the length can be extended easily by replacing the ethynylene groups with higher analogues. The most important attribute of this connector, however, is its reluctance to promote through-bond electron transfer, which is in marked contrast to polyacetylene bridges.[28,29] There is no indication that the connector possesses low-energy excited states that participate in the overall photoprocesses. Instead, we are

(26) (a) Heitele, H.; Finckh, P.; Weeren, S.; Pollinger, F.; Michel-Beyerle, M. E. *J. Phys. Chem.* **1989**, *93*, 5173. (b) Wasielewski, M. R.; Johnson, D. G.; Svec, W. A.; Kersey, K. M.; Minsek, D. W. *J. Am. Chem. Soc.* **1988**, *110*, 7219. (c) Harriman, A.; Heitz, V.; Ebersole, M.; van Willigen, H. *J. Phys. Chem.* **1994**, *98*, 4982.

(27) (a) Shreve, A. P.; Trautman, J. K.; Owens, T. G.; Albrecht, A. C. *Chem. Phys.* **1991**, *154*, 171. (b) Shreve, A. P.; Trautman, J. K.; Owens, T. G.; Albrecht, A. C. *Chem. Phys. Lett.* **1991**, *178*, 89.

of the opinion that such Pt^{II} bis-σ-acetylide units could be important building blocks for construction of artificial light-harvesting arrays where it is important to avoid complications from competing electron transfer.

Acknowledgment. We thank Johnson-Matthey PLC for their generous loan of precious metal salts. Financial support from the Royal Society of London, the CNRS, and ECPM is gratefully acknowledged. We thank Professor Hans Lami for providing important spectroscopic facilities.

Supporting Information Available: Full experimental details regarding the synthesis and characterization of all new compounds, methodology used to derive the photophysical properties and various rate constants, details about the Förster calculations, and a description of the electrochemical setup (PDF). This material is available free of charge via the Internet at http://pubs.acs.org.

JA982300A

(28) (a) Stiegman, A. E.; Miskowski, V. M.; Perry, J. W.; Coulter, D. R. *J. Am. Chem. Soc*. **1987**, *109*, 5884. (b) Khundkar, I. R.; Stiegman, A. E.; Perry, J. W. *J. Phys. Chem*. **1990**, *94*, 1224.

(29) (a) Grosshenny, V.; Harriman, A.; Ziessel, R. *Angew. Chem., Int. Ed. Engl*. **1995**, *34*, 2705. (b) Benniston, A. C.; Harriman, A.; Grosshenny, V.; Ziessel, R. *New J. Chem*. **1997**, *21*, 405.